CONCRETE LIBRARY OF NO. JSCE 13. JUNE 1989

TENSION CRACKING BEHAVIOR OF REINFORCED CONCRETE BEAM BRIDGES

(Translation from Proceedings of JSCE, Vol.390/V-5, February 1988)

Yoshio Ozaka　　Kouji Otsuka　　Yoshinobu Matsumoto

SYNOPSIS

Studies were carried out to investigate the cracking properties of the tension zones of actual RC bridges. Crack spacings and crack widths of three different types of RC bridges were measured and statistically examined. Experiments using RC specimens were also carried out to evaluate the influences of tension and drying.

The spacing and the width in bending zone of actual RC bridges conform well to logarithmic normal distribution. A relation $W_{0.95}$ (95% fractile in the distribution of crack width)=aL+b was observed. Where a and b are coefficients and L is crack spacing. And according to the drying of concrete, both a and b increased. A formula giving the maximum crack spacing and maximum crack width of actual RC bridge was proposed.

Yoshio Ozaka is a professor of structural engineering at Tohoku University, Sendai, since '72. Received his Doctor of Engineering Degree in '72 from his almamater. Senior Engineer, Structures Design Office, Japanese National Railways since '55. MEMBERSHIPS: Delegation of Japan to CEB; Commission "Seismic Design" of FIP; ACI; IABSE; JSCE; JCI; JPCEA. Interested in anti-seismic behavior and cracking property of concrete structure and structural safety problem.

Kouji Otsuka is a professor of civil engineering at Tohoku Gakuin University, Sendai, Japan. He received his Doctor of Engineering Degree from the University of Tohoku in 1981. His research interest is in bond and cracks of reinforced concrete members. He is a member of JSCE, JCI, IABSE, ACI and CEB.

Yoshinobu Matsumoto is a professor of civil engineering at Tohoku Gakuin University, Sendai, Japan. He received his Doctor of Engineering Degree from the University of Tohoku in 1989. His research interest is in shrinkage and crack behavior of reinforced concrete structures. He is a member of JSCE and JCI.

1.INTRODUCTION

It is important to evaluate the crack width which forms in the tensile region of a concrete member for the verification of the serviceability limit state in the design of reinforced concrete (RC) structures. Various kinds of equations have been proposed as the evaluation formulae of crack width. Most of these formulae are, however, derived only from some experimental results in laboratories or theoretical studies because the detailed investigation on cracks in actual RC structures on site is quite difficult.

The properties of cracks in the tensile region of the members in actual structures are greatly affected not only by applied forces but also by various environmental actions such as the direct sunshine, wind, drying , the alternation of drying and wetting, and complex combinations of these actions, so the properties of cracks obtained from tests of specimens in laboratories are quite different from those of cracks in actual structures. Authors revealed in a previous paper[1] that the distribution of cracks becomes polarized when the drying continues long. Therefore, it is necessary to obtain a practical evaluation formula for crack width which was examined by comparing the results of long period measurements on the cracks in actual RC members for at least several years and the test results of factor-controlled specimens in the laboratory.

From the above-mentioned point of view, this paper presents the results of comparison between the analyzed data of cracks in the tensile region of several types of RC girder bridges in comparatively simple stress conditions which are selected from actual RC structures and the results on the RC specimens which have been studied by the authors in the laboratory.[1]~[3]

2.MEASURED BRIDGES AND CRACK MEASURING METHOD

Fig. 1 shows the cross-sections and dimensions of RC girder bridges which were measured for cracks. The characteristics of these bridges are shown in Table 1. The bridges A and B are bridges on the Shinkansen-line and the bridge C is one on a narrow-gage-line. The design procedures of all of these bridges follow the Standard Specification for the Design of Railway Structures of Japanese National Railways. The bridges A and B are constructed in Morioka area and the bridge C is in Sendai area. The environmental conditions of these areas are all rated as the "Normal Environment." The cracks on the bottom and both side surfaces of all of the girders in these bridges are measured at every width-alternating-point using mainly the crack-scale.

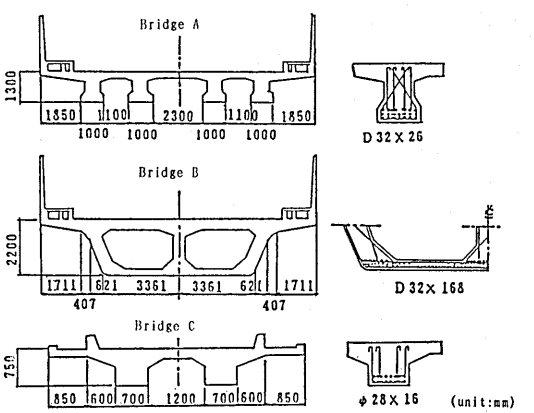

Fig. 1 Cross-sections of measured bridges

Table 1 Characteristics of Measured Bridges

Name	Type of Section	Type of Support	Constructed on	Span Length (m)	Height (m)	Properties of Concrete			Longitudinal Reinforcements				Stirrups	
						σ_{ck} kg/cm^2	W/C	Slump	Designation	Arrangement cm	σ_{sd}	σ_{sl}	Designation	Arrangement cm
A	T-sec.	Simple	July '76	14.10	1.30	240	0.52	12 cm	SD35, D32	C=6.6, Cϕ=8.4	1060	490	SD35, D16	C=5, ctc=25
B	Box-sec.	Simple	Dec. '78	24.08	2.20	270	0.53	10 cm	SD35, D32	C=6.6, Cϕ=7.8	1340	430	SD35, D19	C=5, ctc=12.5
C	T-sec.	Simple	'60	7.00	0.75	200			SS41, ϕ28	C=6.5, Cϕ=7.8	460	940	SS41, ϕ13	C=5.2, ctc=20

Remarks C:cover, Cϕ:Bar spacing, σ_{sd}:Stress in reinforcement at design dead load applied, σ_{sl}:Stress in reinforcement at design live load applied

A dynamic extensometer was used for the measurement of crack width under the live load (only in the case of the bridge A).

The measurements were done as follows:

Bridge A: The first measurement was made two years after the concrete placing and prior to the passing of the first train (called the "second-year-pre measurement"). The second measurement was made approximately six years after the concrete placing and after the train loads had been imposed (called the "sixth-year measurement").

Bridge B: The first measurement was made approximately eight months after the concrete placing and prior to the passing of the first train (called the "eighth-month-pre measurement"). The second measurement was made approximately five years after the concrete placing and after the train load had been imposed (called the "fifth-year measurement").

Bridge C: Only one measurement was made approximately 14 years after the concrete placing and the train load had been imposed.

3. GENERAL TENDENCY OF PROPERTIES OF CRACKS

(1) Crack Pattern

Fig. 2 shows an example of crack pattern of the outer girder in the bridge A at the sixth-year measurement. Most of the cracks formed on the side surfaces in the tensile region of the girder are inclined 45 to 60 degrees to the longitudinal axis of the member within the range of 1.5d (d: the effective depth of the girder) from the support, and perpendicular to the axis where they deviated by more than approximately 3d from the support.

Fig. 3 shows an example of crack pattern which is obtained in the bridge B at the eighth-month-pre measurement. The crack spacings on one side of the box-girder are relatively small comparing with those of the above-mentioned T-section girder (the bridge A). It is also observed that there are numerous parallel cracks which developed across the bottom surface of the bridge almost perpendicular to the longitudinal axis of the member.

Fig. 4 shows the crack pattern of the bridge C. In this case, the crack spacing is large comparing with the other two bridges. This is conceivably because plain bars are used as the longitudinal reinforcement while the other two bridges use deformed bars.

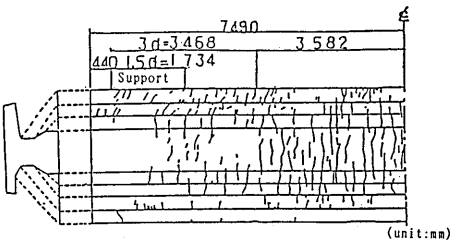

Fig. 2 Example of crack pattern in bridge A (at sixth-year measurement)

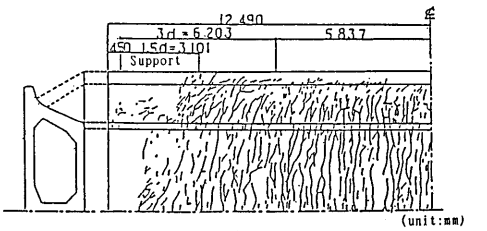

Fig. 3 Example of crack pattern in bridge B (at eighth-month-pre measurement)

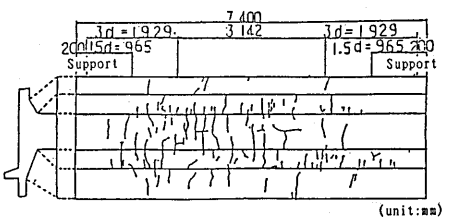

Fig. 4 Example of crack pattern in bridge C

(2) Crack Distribution in Longitudinal Direction

a) Bridge A

Fig. 5 shows the variation in the number of cracks on every one meter section in the longitudinal direction, n, (called the "crack density") and in the mean crack width on the same section, w (called the "mean crack width in one meter") in the longitudinal direction of the inner and outer girders. The crack density and the mean crack width in one meter become gradually large in accordance with the distance from the support toward the midspan. These variations seem to correspond to the magnitude of bending moment in the girder. The rate of variation, however, tends to become considerably small from a/d ((distance from a support)/(effective depth))=3.5 toward the midspan, though with some dispersion. Although both the crack density and the mean crack width in one meter of the outer girders are a little larger than those of inner girders, the variations along the longitudinal axis of these girders are very similar.

Fig. 6 shows an example of the results on the total number of the cracks which cross the lines parallel to the longitudinal axis of the member,N (called the "number of cracks in the flexural region"), the mean crack width, W_m, the mean crack spacing, L_m (called the "mean crack spacing in the flexural region") at the sixth-year measurement excluding both ends of a/d<3.5 from the girder. It follows from the figure that L_m becomes larger in accordance with the distance from the bottom surface toward the neutral axis(② in Fig.6). However, there is little difference in W_m between the bottom surface and the lower flange of side surfaces. Moreover, W_m is not so small in web as expected from the increment of crack spacing and the distribution of flexural strains. This is conceivably because the reinforcement has hardly any effect of confining the drying shrinkage in web.

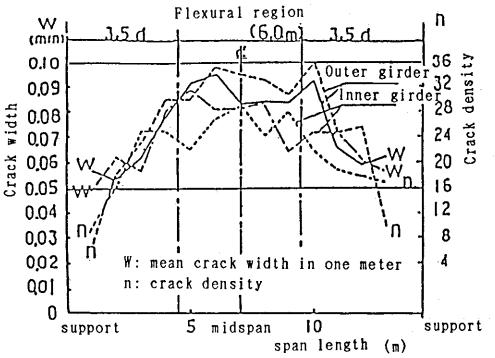

Fig. 5 Variation of cracks in longitudinal direction of bridge A

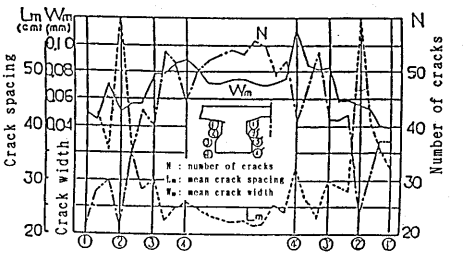

Fig. 6 N,L_m, and W_m on cross-section in flexural region of bridge A

b) Bridge B

Fig. 7 shows the variations in the crack density, n, and the mean crack width in one meter, w, in the longitudinal direction of the bridge B at eighth-month-pre measurement. Both the crack density and the mean crack width in one meter gradually increase in accordance with the distance from the support toward the midspan. The increment is mild comparing with the case of the bridge A. In the flexural region, it may be said that the values are almost constant even in this case.

Fig. 8 shows the number of cracks, N, and the mean crack width, W_m, the mean crack spacing, L_m, in the flexural region (the 9.6m section at midspan). They are obtained by the same method as shown in Fig.6. The relations between the bottom and side surfaces of the girder are quite similar to those of the bridge A. Although they have some dispersion, it is worth noting that the number of cracks is larger and the crack spacing is smaller in the region of large effective reinforcing ratio (at both sides ③ and center ⑤) than in the region of small ratio (mid part ④) on the broad bottom surface.

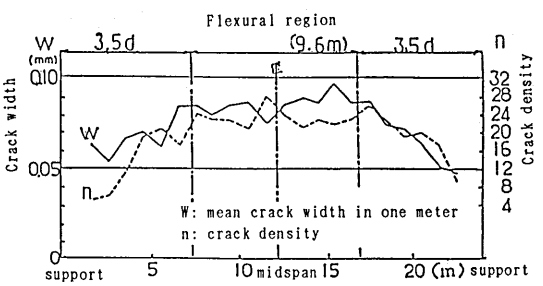

Fig. 7 Variation of cracks in longitudinal direction of bridge B

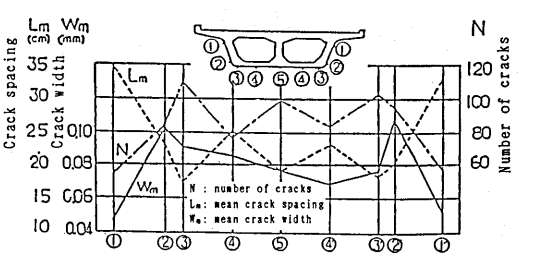

Fig. 8 N, L_m, and W_m on cross-section in flexural region of bridge B

c) Bridge C

Fig. 9 shows the variations in the crack density, and the mean crack width on one meter section, w, in the longitudinal direction. Even in this case, the

values may be regarded as being constant in the flexural region. It is especially noteworthy that any decrease in the mean crack width in one meter, w, was not observed within the outside section of the flexural region, unlike the cases of bridges using the deformed reinforcing bars.

Fig. 10 shows the number of cracks, N, the mean crack width, W_m, and the mean crack spacing, L_m, in the flexural region on the cross-section of the girder. The general tendency is almost the same as in the bridge A.

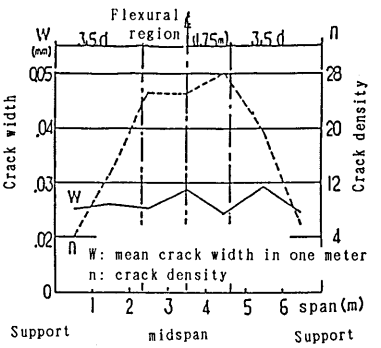

Fig. 9 Variation of cracks in longitudinal direction

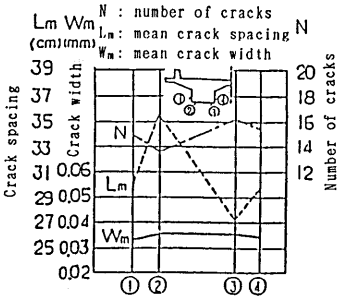

Fig. 10 N, L_m, and W_m on cross-section in flexural region of bridge C

4.STATISTICAL ANALYSIS ON CRACKS IN FLEXURAL REGION

(1) Crack Spacing

a) Bridge A

Figs. 11 and 12 show the frequency distribution of crack spacings in all the eight girders of the bridge A at the second-year-pre measurement in the position of the extreme longitudinal reinforcing bar on the bottom surface (called the "outside-bottom layer"), and in the position of the bottom longitudinal reinforcing bars on the side surface (called the "bottom-side layer"), respectively. It should be noted that this frequency distribution conforms not to the conventionally predicted normal distribution but to the logarithmic-normal distribution. The two dotted lines give respectively the distribution curves of four outer girders and four inner girders.

According to the findings by the authors[1] using the axially tensioned RC specimens, the crack spacing conforms to the logarithmic-normal distribution in the case of moist specimens. The pattern of the distribution, however, is fairly close to the normal distribution. On the contrary, in the case of dried specimens, the pattern becomes polarized, and it fits nothing but the logarithmic-normal distribution. This is conceivably because small-spacing cracks increase in number with the progressive drying of concrete and the crack spacing does not assume a negative value.

There are no significant differences in the distribution patterns and in the mean values of crack width among all the eight girders between their bottom and side surfaces. The number of cracks in the flexural region, N, is larger and the mean crack spacing in the same region, L_m, is smaller than those of inner girders in all cases. These tendencies are conspicuous on the bottom surface. This is conceivably because the outer girders receive much influence of rain and direct sunshine.

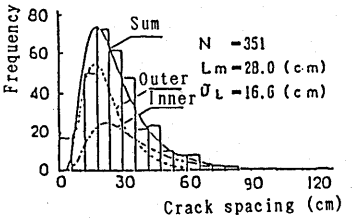

Fig. 11 Distribution of crack spacing on outer-bottom layer in bridge A (at second-year-pre measurement)

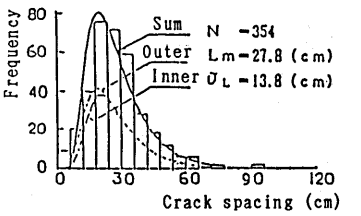

Fig. 12 Distribution of crack spacing on bottom-side layers in bridge A (at second-year-pre measurement)

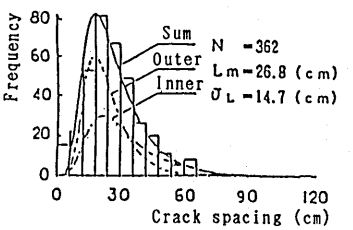

Fig. 13 Distribution of crack spacing on outer-bottom layer in bridge A (at sixth-year measurement)

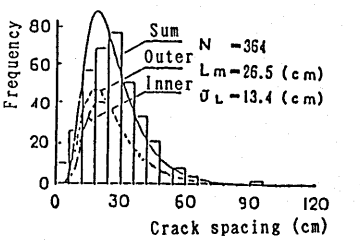

Fig. 14 Distribution of crack spacing on bottom-side layers in bridge A (at sixth-year measurement)

Figs. 13 and 14 show the distribution of the crack spacings in all the eight girders on the outside-bottom layer and the bottom-side layers in the flexural region of the bridge A at the sixth-year measurement. The dotted lines give the distribution curves of four outer girders and four inner girders. Table 2 shows the number of cracks in the flexural region, N; the crack spacing in the same region, L_m; the standard deviation, and the crack spacing at the probability of five percent excess, $L_{0.95}$, at the second-year-pre measurement and the sixth-year measurement. From these figures, it follows that there are little differences in the distribution pattern except that N is slightly large (approximately three percent) and L_m is slightly small (approximately three percent) at the sixth-year measurement. It may be interpreted that this change in the properties of cracks between the second-year-pre measurement and the sixth-year measurement reflects the train loading history of four years and the alternation of drying and wetting.

Table 2 Measured Crack Spacing of Bridge A

		N			L_m cm			σ_L cm			$L_{0.95}$ cm		
		Outer girder	Inner girder	Sum	Outer girder	Inner girder	Sum	Outer girder	Inner girder	Sum	Outer girder	Inner girder	Sum
Second-Year-Pre Measurement	Bottom	207	144	351	23.8	33.6	28.0	12.0	19.5	16.6	46.0	69.9	58.5
	Side	182	172	354	26.9	28.7	27.8	13.9	13.7	13.8	52.7	54.1	53.4
Sixth-Year-Measurement	Bottom	209	153	362	23.1	31.9	26.8	10.5	17.7	14.7	42.5	64.8	54.1
	Side	189	175	364	25.3	27.7	26.5	13.1	13.6	13.4	49.5	53.0	51.3

Remarks N:Number of cracks in the flexural region, L_m:Mean crack spacing in the flexural region, σ_L:Standard deviation
$L_{0.95}$:Maximum value of 95%

b) Bridge B

Fig. 15 shows the distribution of the crack spacings in the flexural region, L, at outside-bottom layer (solid line) and bottom-side layers (dotted line) of the bridge B at the eighth-month-pre measurement. In the case of box-girder, the distribution pattern differs between the bottom surface and the side surfaces. The mean value and the standard deviation of the bottom surface are smaller by approximately 18 percent and 29 percent, respectively.

Figs. 16 and 17 show the distribution of crack spacings at the fifth-year measurement (solid line) and the eighth-month measurement (dotted line) within the three meters section at midspan in the flexural region of the bridge B.

Table 3 shows the number of cracks, N, the mean crack spacing, L_m, the standard deviation, and the crack spacing at the probability of five percent excess, $L_{0.95}$, in the flexural region at the eighth-month measurement, on three-meter section at midspan at the eighth-month measurement, and on three-meter section at midspan at the fifth-year measurement. Comparing the results of eighth-month measurement and the fifth-year measurement, 9.3 percent increase in N on the outside-bottom layer and 16.2 percent increase on the bottom-side layers are observed. There are 9.0 percent decrease in L_m on the outside-bottom layer and 15.3 percent decrease on the bottom-side layers. There are also 4.7 percent decrease in $L_{0.95}$ and 23.2 percent decrease on the bottom-side layers. They are interpreted to indicate that the crack gradually increases in number as a result of the repetition of train loading and the alternation of drying and wetting of concrete.

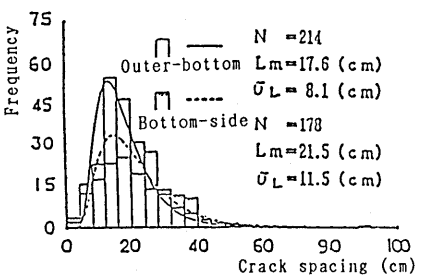

Fig. 15 Distribution of crack spacing on outer-bottom and bottom-side layers in bridge B (at eight-month-pre measurement)

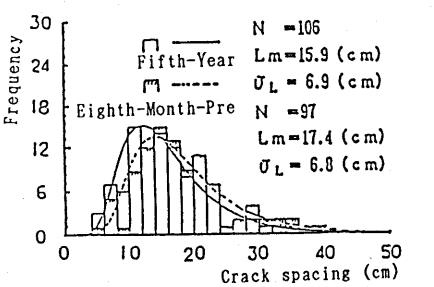

Fig. 16 Distribution of crack spacing on outer-bottom layer in bridge B (midspan 3m section)

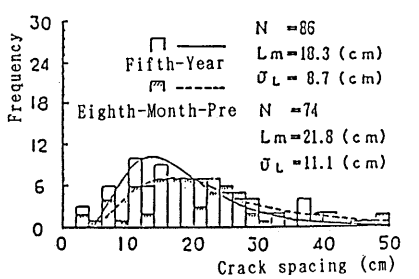

Fig. 17 Distribution of crack spacing on bottom-side layer in bridge B (midspan 3m section)

Table 3 Measured Crack Spacing of Bridge B

		N	L_m cm	σ_L cm	$L_{0.95}$cm
Eighth-Month-Pre Measurement	Bottom	214	17.6	8.11	32.2
	Side	178	21.5	11.46	42.8
Eighth-Month-Pre Measurement (midspan 3m)	Bottom	97	17.4	6.82	30.1
	Side	74	21.8	11.12	42.3
Fifth-Year Measuremnt (midspan 3m)	Bottom	106	15.9	6.93	28.7
	Side	86	18.3	8.70	32.5

c) Bridge C

Fig. 18 shows the crack spacing in the flexural region of the bridge C on the bottom and side surfaces. As plain bars are used in the bridge C unlike the bridges A and B, the dispersion of crack spacings is quite large. The mean crack spacing on the side surfaces is a little larger than on the bottom surface.

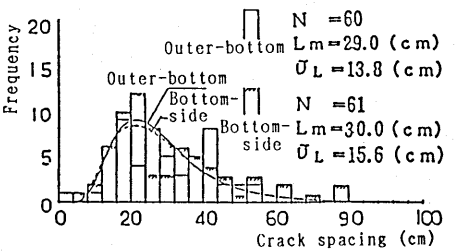

Fig. 18 Distribution of crack spacing on outer-bottom and bottom-side layers in bridge C

(2) Crack Width

a) Bridge A

Figs. 19 and 20 show the crack width respectively on the outside-bottom layer and on the bottom-side layers in the flexural region at the second-year measurement. The solid line shows the distribution curve of all the eight girders and the dotted lines show those of four outer girders and four inner girders. They have larger dispersions comparing with the case of crack spacing because of the inherent errors of the crack gage readings. The distribution pattern conforms not to the conventionally predicted normal distribution but to the logarithmic-normal distribution. There are little differences in the mean value and the standard deviation of crack width in the flexural region of all the eight girders between the bottom surface and side surfaces. Many of the outer girders have larger modes and crack widths than those of the inner girders. As shown in 4.(1), the outer girders had a tendency to have a larger number of cracks in the flexural region, N, and smaller mean crack spacings in the flexural region, L_m. The tendency is interpreted as indicating that the outer girders bear larger dead weights and suffer severe influence of drying and wetting under direct sunlight and rain.

Figs. 21 and 22 show the distribution of crack widths in the flexural region on the outside-bottom layers and the bottom-side layers of all the eight girders at the sixth-year measurement.

Table 4 shows the number of cracks, N, the mean crack width, W_m, the standard deviation and the crack width at the probability of five percent excess, $W_{0.95}$ in the flexural region at the second-year-pre measurement and sixth-year measurement.

From the above, it is seen that N increases a little (three percent) both on the outside-bottom layer and on the bottom-side layers from the second-year measurement to the sixth-year measurement. On the contrary, W_m increases 19 percent on the outside-bottom layers and 12 percent on the bottom-side layers. This is a remarkable phenomenon.

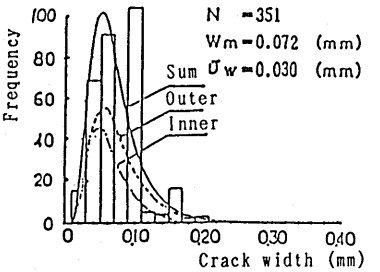

Fig. 19 Distribution of crack width on outer-bottom layer in bridge A (at second-year-pre measurement)

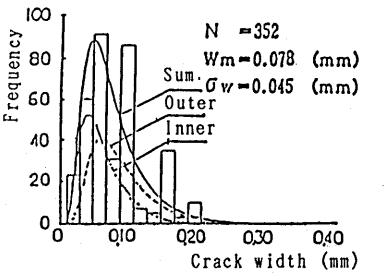

Fig. 20 Distribution of crack width on bottom-side layers in bridge A (at second-year-pre measurement)

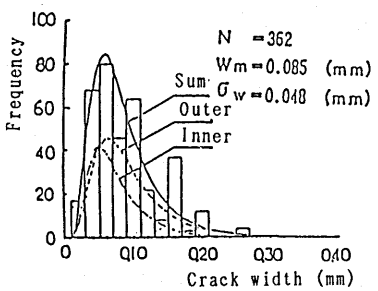

Fig. 21 Distribution of crack width on outer-bottom layer in bridge A (at sixth-year measurement)

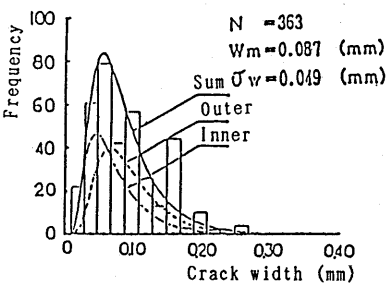

Fig. 22 Distribution of crack width on bottom-side layers in bridge A (at sixth-year measurement)

Table 4 Measured Crack Width of Bridge A

		N			W_m mm			σ_w mm			$W_{e.95}$ mm		
		Outer girder	Inner girder	Sum	Outer girder	Inner girder	Sum	Outer girder	Inner girder	Sum	Outer girder	Inner girder	Sum
Second-Year-Pre Measurement	Bottom	207	144	351	0.077	0.066	0.072	0.0399	0.0332	0.0369	0.15	0.13	0.14
	Side	181	171	352	0.090	0.065	0.078	0.0497	0.0368	0.0458	0.18	0.13	0.16
Sixth-Year-Measurement	Bottom	209	153	362	0.093	0.075	0.085	0.0509	0.0426	0.0484	0.19	0.16	0.18
	Side	188	175	363	0.099	0.074	0.087	0.0502	0.0442	0.0490	0.19	0.16	0.18

Remarks N:Number of cracks in the flexural region, W_m:Mean crack width in the flexural region, σ_w:Standard deviation
$W_{e.95}$:Maximum value of 95%

The length and depth of cracks had increased and the rigidity of the member had decreased with an increase in the number of cracks due to the repeated application of train load. The effect of drying of concrete in four years is supposed to have a great influence on them. Comparing the outer and inner girders, both the outside-bottom layer and the bottom-side layers of the outer girders had a larger number of cracks and a larger mean crack width at both the second-year-pre measurement and the sixth-year measurement. The difference in the mean crack widths slightly decreased on the side surfaces and greatly increased on the bottom surface.

Fig. 23 shows samples of measured fluctuations of crack width on the bottom of girders. They are measured at the midspan(Point 11), the quarter point of the span (Point 10), and near the support (Point 12) within a same girder. The train had 12 cars and ran approximately at 180 km/h.

Table 5 shows the values of the measured crack widths under the application of dead loads and live loads. The crack width increases approximately by 0.01 to 0.02 mm at the midspan under the passing of train. This corresponds to approximately 30 MPa of the calculated increment of stress in reinforcement. (This value is computed taking the load as shown in Fig.23, the impact factor as 0.15, and the cross-section as shown in Fig.1). The reason why the crack width increases only 10 to 20 percent at the midspan under the train load is an enlarged rigidity due to the existence of the slab track and road-bed concrete.

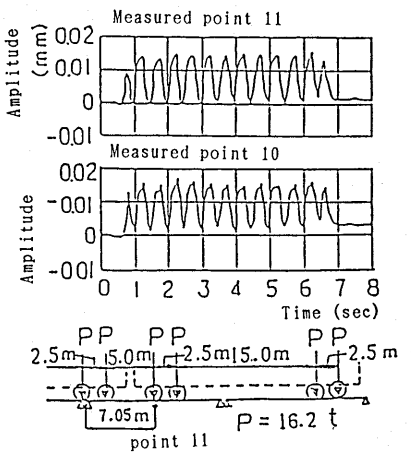

Fig. 23 Measured fluctuations of crack width under live load

Table 5 Dynamic Measurement Results of Crack Width

	No.	Distance from the support	Crack Width (mm)		
			W_d	W_l	$W_d + W_l$
Outer Girder No. 1	1	1.05	0.10	0.003	0.103
	2	4.01	0.15	0.009	0.159
	3	7.29	0.15	0.010	0.160
	4	12.87	0.10	0.004	0.104
Inner Girder No. 2	5	1.07	0.10	0.002	0.012
	7	7.39	0.10	0.017	0.117
	8	12.30	0.15	0.004	0.154
Inner Girder No. 3	10	4.45	0.08	0.019	0.099
	11	7.05	0.15	0.014	0.164
	12	12.63	0.20	0.003	0.203
Outer Girder No. 2	13	1.78	0.25	0.004	0.254
	15	7.05	0.15	0.011	0.161

b) Bridge B

Fig. 24 shows the distribution of crack widths on the bottom surface and the side surface in the flexural region at the eighth-month-pre measurement. From this figure, it is seen that the side surfaces have a larger dispersion of crack widths, approximately 20 percent smaller number of cracks, and approximately 20 percent larger mean crack width than the bottom surface.

Fig. 25 shows the distribution of crack widths respectively on the outside-bottom layer and on the bottom-side layers within the mid three-meter-section in the 9.6 meter flexural region at the fifth-year measurement. For comparison, the distribution of crack widths in the same region at the eight-month measurement is shown using a dotted line.

Table 6 shows the number of cracks, N, the mean crack width, W_m, the standard deviation, and $W_{0.95}$ in the flexural region at the eighth-month-pre measurement, on the mid-three-meter section at the eighth-month-pre measurement, and on the mid-three-meter section at the fifth-year measurement.

From the above, it is seen that N increased 9.2 percent on the outside-bottom layer and 17.8 percent on the bottom-side layers, W_m increased 38.4 percent on the outside-bottom layer and 12.8 percent on the bottom-side surfaces in the period from the eighth-month-pre measurement to the fifth-year measurement on the same mid-three-meter section. Also, $W_{0.95}$ increased 23.7 percent on the outside-bottom layer and 8.1 percent on the bottom-side layers. The reason for the smaller increase of the crack width on the bottom-side layers than on the outside-bottom layer seems to be that the increase in the number of cracks is large on the side surfaces. In all cases, the increase in the crack width in the period from the eighth-month-pre measurement to the fifth-year measurement is obvious. This is because the train loading history and continued drying of concrete in four years had great influences.

c) Bridge C

Fig. 26 shows the distribution of crack widths on the outside-bottom layer and the bottom-side layers in the flexural region. Although the distribution includes a great dispersion, the mean crack width on the bottom-side layers is approximately 3.5 percent smaller than on the outside-bottom layer.

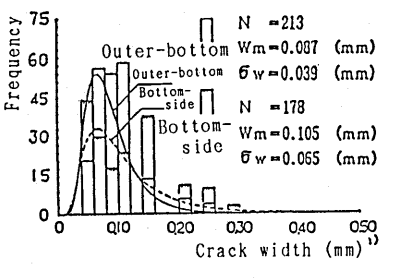

Fig. 24 Distribution of crack width on outer-bottom and bottom-side layers in bridge B (at eighth-month-pre measurement)

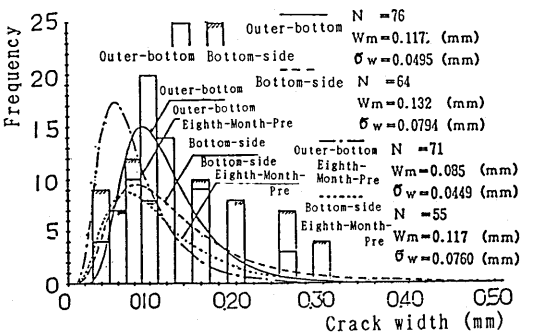

Fig. 25 Distribution of crack width on outer-bottom and bottom-side layers in bridge B (midspan 3m section)

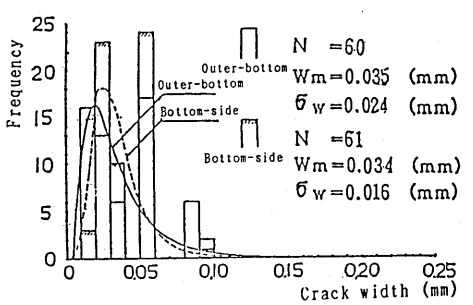

Fig. 26 Distribution of crack spacing on outer-bottom and bottom-side layers in bridge C

Table 6 Measured Crack Width of Bridge C

		N	W_m mm	σ_w mm	$W_{0.95}$mm
Eighth-Month-Pre Measurement	Bottom	213	0.087	0.0398	0.161
	Side	178	0.105	0.0652	0.227
Eighth-Month-Pre Measurement (midspan 3m)	Bottom	71	0.085	0.0449	0.169
	Side	55	0.117	0.0760	0.259
Fifth-Year Measurement (midspan 3m)	Bottom	76	0.117	0.0495	0.209
	Side	64	0.132	0.0794	0.280

(3)Skewness of Distributions of Crack Spacings and Crack Widths

As described before, it is clear that the distributions of crack spacings and widths in the tensile region of members in actual bridges are polarized with lapse of time under the environmental conditions. As the main cause for this, the drying of concrete can be mentioned. Therefore, the crack spacing and width were observed using several drying prismatic test specimens in order to determine the fundamental properties. The shape of specimen was a rectangular prism (6cm*6cm*180cm) with reinforcing bar (D16) placed at the centroid axis. The specimens had been water cured and kept on a shelf in a constant-temperature and constant-moisture room (20°C,RH=50%) until they came to have the prescribed moisture content. The drying process of the specimens was monitored with a specimen placed under the same drying condition (the same cross-section and the length 30cm). After 10 repetitions of loading up to 2,000 kgf/cm^2 of the stress in reinforcement, the crack width was measured using a microscope or a contact-type strain-meter on the centroid axis of the specimen keeping the stress of reinforcing bar at 2,000 kgf/cm^2.

Fig. 27 shows the distribution of crack spacings and Fig.28 shows the distribution of crack widths. Tables 7 and 8 show the results of statistical analysis of crack spacing and crack width, respectively. Fig. 29 shows the relationship between $L_{0.95}$, L_{mo} and the water content in percent of total weight (ω). Fig. 30 shows the relationship between $W_{0.95}$, W_{mo} and the water content in percent of total weight. As for the crack spacing, $L_{0.95}$ and L_{mo} increase slightly with a decrease of the water content in percent of total weight in the concrete of specimen, but (L_m-L_{mo}), ($L_{0.95}$-L_{mo}) and degree of skewness ((the third order moment around the mean value)/(the third power of the standard deviation), α_3, do not change. In crack width, there are little differences between wet condition (ω =7.65%) and slightly dried condition (ω =5.31%). The distribution is polarized and the degree of skewness becomes large according to the degree of drying. Fig. 31 shows an example of the degree of skewness in the distribution of crack widths.

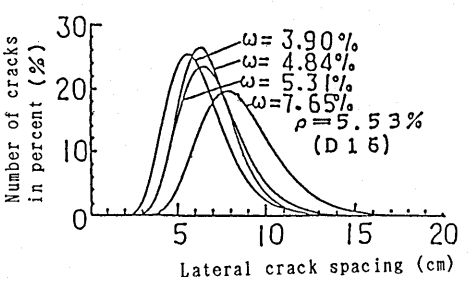

Fig. 27 Variation of lateral crack spacing in axially tensioned specimens

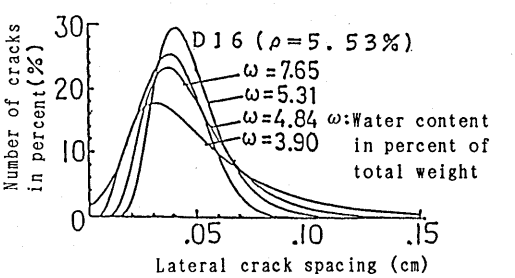

Fig. 28 Variation of lateral crack width in axially tensioned specimens

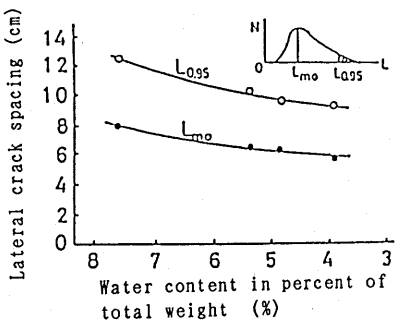

Fig. 29 Relation between lateral crack spacing and water content in percent of total weight for axially tensioned specimens

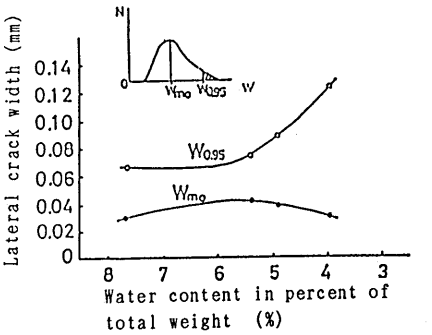

Fig. 30 Relation between lateral crack width and water content in percent of total weight for axially tensioned specimens

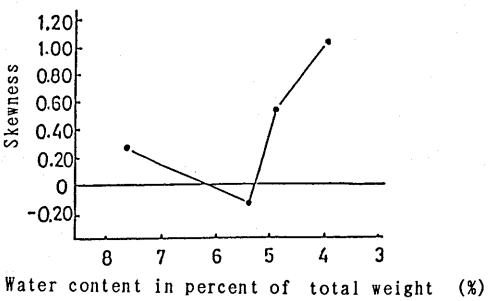

Fig. 31 Relation between skewness of lateral crack spacing and water content in percent of total weight of axially tensioned specimens

Table 7 Representative values, dispersion (cm) and skewness of crack spacing distribution for axially tensioned specimens

		N	L_m	$L_{0.95}$	L_{mo}	$L_m - L_{mo}$	$L_{0.95} - L_{mo}$	σ_L	α_{3L}
Water Content in Percent of Total Weight	7.65	258	8.57	12.5	7.79	0.78	4.71	2.212	0.137
	5.31	128	7.04	10.3	6.38	0.66	3.92	1.833	-0.183
	4.84	146	6.77	9.6	6.23	0.54	3.37	1.614	0.079
ω %	3.90		6.18	9.2	5.53	0.65	3.67	1.717	0.136

Table 8 Representative values, dispersion (mm) and skewness of crack width distribution for axially tensioned specimens

		N	W_m	$W_{0.95}$	W_{mo}	$W_m - W_{mo}$	$W_{0.95} - W_{mo}$	σ_w	α_{3w}
Water Content in Percent of Total Weight	7.65	33	0.038	0.067	0.030	0.008	0.037	0.0158	0.271
	5.31	125	0.047	0.075	0.040	0.007	0.035	0.0154	-0.193
	4.84	140	0.048	0.088	0.037	0.011	0.077	0.0214	0.536
ω %	3.90	157	0.054	0.121	0.031	0.023	0.090	0.0358	1.030

Tables 9 and 10 show the skewness of the distribution of crack spacings and the skewness of the distribution of crack widths measured in the bridge A. Tables 11 and 12 show the skewness of the distribution of crack spacings and the skewness of the distribution of crack widths measured in the bridge B. As for the bridge A, comparing with the test results of axially tensioned specimens, little changes were observed in the skewness of the distribution of crack spacings depending on the measurement period, but, a tendency of increase was observed in the skewness of the distribution of crack widths corresponding to the degree of drying.

Table 9 Representative values, dispersion (cm) and skewness of crack spacing distribution for bridge A

		N		L_{mo}		L_m-L_{mo}		$L_{0.95}-L_{mo}$		σ_L		σ_{3L}	
		Outer	Inner	Outer	Inner	Outer	Inner	Outer	Inner	Outer	Inner	Outer	Inner
Second-Year-Pre Measurement	Bottom	207	144	16.9	21.7	6.9	11.9	29.1	48.2	12.0	19.5	0.541	1.265
	Side	182	172	18.9	21.1	8.0	7.6	33.8	33.0	13.9	13.7	1.320	0.926
Sixth-Year Measurement	Bottom	209	153	17.4	21.3	5.7	10.6	25.1	43.5	10.5	17.7	0.576	1.214
	Side	189	175	17.7	20.0	7.6	7.7	31.8	33.0	13.1	13.6	1.209	1.058

Remarks; N: Number of cracks, L_{mo}: Mode, L_m: Mean value, $L_{0.95}$: Maximum of 95%, σ_L: Standard deviation, σ_{3L}: Skewness

Table 10 Representative values, dispersion (mm) and skewness of crack width distribution for bridge A

		N		W_{mo}		W_m-W_{mo}		$W_{0.95}-W_{mo}$		σ_W		σ_{3W}	
		Outer	Inner	Outer	Inner	Outer	Inner	Outer	Inner	Outer	Inner	Outer	Inner
Second-Year-Pre Measurement	Bottom	207	144	0.054	0.047	0.023	0.019	0.096	0.083	0.0399	0.0332	0.264	0.687
	Side	181	171	0.060	0.043	0.030	0.022	0.120	0.087	0.0497	0.0368	0.222	0.760
Sixth-Year Measurement	Bottom	209	153	0.063	0.049	0.030	0.026	0.127	0.111	0.0509	0.0426	0.764	1.253
	Side	188	175	0.070	0.047	0.029	0.027	0.120	0.113	0.0502	0.0442	0.563	0.762

Remarks N: Number of cracks, L_{mo}: Mode, L_m: Mean value, $L_{0.95}$: Maximum of 95%, σ_W: Standard deviation, σ_{3W}: Skewness

Table 11 Representative values, dispersion (cm) and skewness of crack spacing distribution for bridge B

		N	L_m	$L_{0.95}$	L_{mo}	L_m-L_{mo}	$L_{0.95}-L_{mo}$	σ_L	α_{3L}
Eighth-Month-Pre Measurement (midspan 3m)	Bottom	97	17.4	30.1	14.0	3.4	16.1	6.82	0.854
	Side	74	21.6	42.3	15.2	6.4	27.1	11.12	2.022
Fifth-Year Measurement (midspan 3m)	Bottom	106	15.9	28.7	12.2	3.7	16.5	6.93	0.877
	Side	86	16.0	32.5	11.2	5.1	21.3	8.70	2.998

Table 12 Representative values, dispersion (mm) and skewness of crack width distribution for bridge B

		N	W_m	$W_{0.95}$	W_{mo}	W_m-W_{mo}	$W_{0.95}-W_{mo}$	σ_W	α_{3W}
Eighth-Month-Pre Measurement (midspan 3m)	Bottom	71	0.085	0.169	0.058	0.027	0.111	0.0449	2.116
	Side	55	0.117	0.259	0.069	0.048	0.190	0.0760	0.736
Fifth-Year Measurement (midspan 3m)	Bottom	76	0.117	0.209	0.092	0.025	0.117	0.0495	0.896
	Side	64	0.132	0.280	0.083	0.049	0.197	0.0794	0.630

The following general tendencies can be recognized through the comparison in the skewness of distributions of crack spacings and widths between the axially tensioned specimens and the actual bridges.

1. The distributions of crack spacings and widths in the tensile region are close to the normal distribution when the concrete is in the moist condition or at the early stage of drying. The skewness is close to zero.

2. The crack spacing becomes smaller beginning from the most sensitive region to the loading condition as the drying condition continues. The skewness becomes large.

3. When the drying further continues, cracks with large spacing develop due to drying even in the region which is the least sensitive to the loading condition. The skewness sometimes becomes slightly small.

(4)Relation between Crack Spacing and Crack Width

As a sample of the relationship between the crack spacing and the crack width, Fig. 32 shows the measured results obtained from the bottom surface in the flexural region of the bridge A at the second-year-pre measurement. As shown here, the relation disperses greatly and is not a simple linear relation like the test results of axially tensioned specimens. The double circles in the figure indicate each point of probability of five percent excess in the distribution of crack widths at every five centimeter crack spacing. (It is confirmed that here also the distribution conforms to the logarithmic-normal distribution.) The straight (solid) line in the figure means that 95 percent of the measured values come below the line (called "95%-confidential line"). The dotted line gives the 95%-confidential line for the fifth-year measurement obtained in the same manner. Considering only the 95 percent maximum crack widths, $W_{0.95}$, of respective crack spacings, the crack spacing is less than approximately 40 cm, and they almost fit the straight line aL+b. The reason why there is no such fitting in the region of large crack spacings is because in this region cracks have not yet settled to a stable condition. It is interesting to point out that both a and b have a tendency to become large at the fifth-year measurement comparing the values between the eighth-month and the fifth-year measurements. This seems to suggest that a part of the loading history and drying of concrete which affects the crack width are related to the crack spacing while the other parts are not.

Figs. 33 and 34 show the 95% confidential lines obtained from the relations between the crack spacing and the crack width respectively on the bottom and side surfaces in the flexural region of the bridge B at the eighth-month measurement and on the bottom surface of the bridge C in the same manner as shown in Fig.32. (The individual measured results are omitted.) The gradient of the 95% confidential line for the bottom surface of bridge C is slightly smaller than on the bridges A and B. This is conceivably because the magnitude of stress in the reinforcement is small.

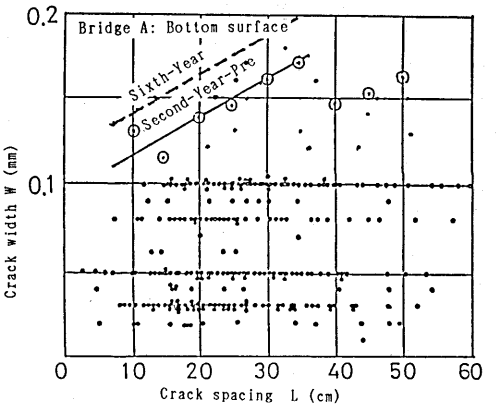

Fig. 32 Relation between crack spacing and crack width (Bridge A)

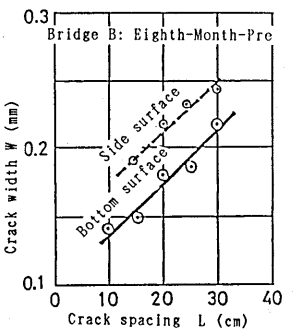

Fig. 33 Relation between crack spacing and crack width (Bridge B)

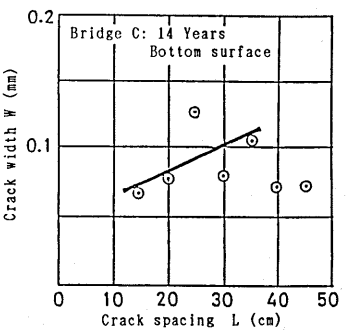

Fig. 34 Relation between crack spacing and crack width (Bridge C)

5.CALCULATION OF CRACK SPACING AND CRACK WIDTH

(1) Calculation of Crack Spacing

The most simplified equation as shown below has been proposed to calculate the maximum crack spacing, L_{max}.

$$L_{max}=K\cdot C \qquad \ldots(1)$$

For the value of K, the authors proposed K=6.0 in a previous paper.[1]

As described in 3.(2), the mean crack spacing tends to become smaller in the region of large steel ratio on the broad bottom surface of a box-girder, so it is necessary to consider the influences of the reinforcing bar spacing (C_ϕ) and the diameter of reinforcing bar (ϕ) besides the steel ratio (ρ_r). Therefore the following equation is obtained adding the terms of these influential factors linearly to Eq.(1).

$$L_{max}=K\{\eta_1 C+\eta_2(C_\phi-\phi)+\eta_3\phi/\rho_r\} \quad \ldots(2)$$

where, K is 1 for deformed bars and 1.3 for plain bars.
Comparing the test results obtained from the axially tensioned specimens and beams with the measured results of actual bridges, η_1=5 and η_2=0.5 are obtained. As the mean crack spacing is approximately 25 percent smaller in the region of large effective steel ratio (10.2%) of the outer part on the bottom surface of the bridge B than in the region of small ratio(5.1%), n $_3$ is taken as 0.1.
Therefore, Eq.(2) becomes as follows.

$$L_{max}=K\{5C+0.5(C_\phi-\phi)+\phi/10\rho_r\} \quad \ldots.(3)$$

Table 13 gives the calculated values of L_{max} and the values of probabilities of excess for e=1 to 7 percent which are obtained from the measured crack spacing ($L_{0.99}$ ~ $L_{0.93}$) for the bridges A, B, and C. As the formula in CEB gives the mean crack spacing, L_{max} was obtained as $L_{max}=1.7S_{rm}$.

There are approximately at most 30 percent differences in L_{max} among the four equations. The relation between the calculated values and measured values varies somewhat with the bridges. For bridge A, all the equations except Eq.(3) give smaller values than $L_{0.93}$. For bridge B, the values obtained by Eq.(3) are close to $L_{0.97}$ on the bottom surface and $L_{0.93}$ on the side surfaces. For bridge C, which uses plain bars, the equations except Eq.(3) give much smaller values than measured values. This implies that Eq.(3) is superior to the other equations.

Table 13 Maximum Crack Spacing, L_{max}

			Measured values (cm)				Calculated values (cm)			
			e				Kakuta Eq.	CEB-FIP Eq.	JSCE Eq.	Proposeed Eq.
			1%	3%	5%	7%				
Bridge A	Bottom	Outer	57.1	47.1	42.5	39.6	35.6	30.4	32.9	42.1
		Inner	92.4	73.3	64.9	59.4				
		Sum	76.7	61.1	54.2	49.6				
	Side	Outer	69.1	55.7	49.7	45.7				
		Inner	72.7	59.5	53.2	49.2				
		Sum	71.1	57.6	51.3	47.4				
Bridge B	Bottom	Sum	44.0	36.2	32.6	30.3	35.6	27.8	29.2	38.5
	Side	Sum	60.2	48.2	42.8	39.3				
Bridge C	Bottom	Sum	74.4	60.8	54.6	50.6	----	32.0	38.4	51.0
	Side	Sum	82.6	66.3	59.0	54.3				

Formula proposed by Kakuta	CEB-FIP Formula	JSCE Formula
Lmax=KC in the case es/C>2.5	Srm= $\frac{2(C+C\phi/10)+K1K2\Phi/\rho_r}{}$	Lmax= K1(4C+0.7(Cφ-Φ)
Lmax= $\frac{KC}{1.45}(1+0.18\frac{es}{C})$	where, Srm: mean crack spacing K1=0.4 (for deformed bars) K1=0.8 (for plain bars) K2=0.125 (for pure bending) K2=0.25 (for pure tension)	where, K1=1 (for deformed bars) K2=1.3 (for plain bars) C : concrete cover Cφ: re-bar spacing Φ : bar diameter

(2) Calculation of Crack Width

It is generally understood that there is a linear relation between the crack width and the crack spacing in the stable cracking condition. However, as mentioned in 4.(4), there are no clear relations between the crack width and the crack spacing in actual bridges because of great dispersion. Only a linear relation of $W_{max}=aL+b$ can be observed between the maximum crack width, W_{max}, corresponding to a certain crack spacing and the crack spacing. The values of a and b depend on the stress in reinforcement, loading history and drying condition of concrete of each member. From this, it is conceivable that influence of the drying condition on W_{max} can be divided into two parts, one related, and one unrelated, to L. The former is the influence of a constant drying shrinkage on concrete surface and inside of concrete. The latter is the influence of a larger drying shrinkage than inside of concrete, which occurs on the surface close to the cracks.

Based on the experimental results on the axially tensioned RC specimens, the authors have previously proposed the following equation as a formula for W_{max}[1].

$$W_{max}=\gamma L_{max}(\zeta\sigma_s/E_s-\varepsilon'_{\varphi c}) \\ =kL_{max}(\sigma_s/E_s-\varepsilon_{\varphi c}) \quad \ldots\ldots(4)$$

where, $\varepsilon_{\varphi c}=\varepsilon'_{\varphi c}/\zeta$ $\quad k=\gamma\zeta$ $\quad$ (k=0.6)

The next equation may be derived by adding K_c as an independent term to above-mentioned L in Eq.(4), changing the sign of $\varepsilon_{\varphi c}$, and substituting L_{max} into Eq.(3).

$$W_{max}=K_a(5C+0.5(C_\phi-\phi)+\phi/10\rho_r)(\sigma_s/E_s+\varepsilon_{\varphi c})+K_c \quad \ldots\ldots(5)$$

where, K_a=kK=0.6 : for deformed bars.
K_a=0.8 : for plain bars.

The values of $\varepsilon_{\varphi c}$ and K_c should be altered depending on the conditions of members.

Although L_{max} and W_{max} in Eqs.(3) and (4) ought to be supposed to follow an extremal distribution, here the representative values were obtained by the following examination.

Comparing the test results of axially tensioned RC specimens and the measured results shown in Figs. 32, 33 and 34, these values are selected as follows:

Bridge A: $\varepsilon_{\varphi c}=80*10^{-6}$, K_c=0.008 (cm)
Bridge B: $\varepsilon_{\varphi c}=90*10^{-6}$, K_c=0.010 (cm)
Bridge C: $\varepsilon_{\varphi c}=20*10^{-6}$, K_c=0.004 (cm)

Table 14 shows $W_{0.99}$~$W_{0.93}$ obtained from the calculated values of W_{max} and the measured crack widths. As seen from these results, in general, W_{max} obtained from Eq.(4) can be taken as $W_{0.95}$. The value of $W_{0.95}$ is considered an adequate index to describe the possibility of the corrosion of reinforcing bars.

Table 14 Maximum Crack Width, W_{max}

			Measured values (cm)				Calculated values (cm)			
			e				Kakuta Eq.	CEB-FIP Eq.	JSCE Eq.	Pro-poseed Eq.
			1%	3%	5%	7%				
Bridge A	Bottom	Outer	0.27	0.21	0.19	0.16	0.30	0.10	0.20	0.22
		Inner	0.22	0.18	0.16	0.14				
		Sum	0.25	0.20	0.18	0.16				
	Side	Outer	0.27	0.22	0.19	0.18				
		Inner	0.23	0.18	0.16	0.14				
		Sum	0.26	0.20	0.18	0.16				
Bridge B	Bottom	Sum	0.22	0.18	0.16	0.15	0.28	0.05	0.25	0.27
	Side	Sum	0.34	0.26	0.23	0.21				
Bridge C	Bottom	Sum	0.13	0.10	0.08	0.07	----	0.08	0.15	0.14
	Side	Sum	0.09	0.07	0.07	0.06				

Formula proposed by Kakuta

$Wmax=(\sigma s/Es-\sigma cm/EsPe-\varepsilon)Lmax$

CEB-FIP Formula

$Wmax=1.7Wm$

$Wm=Srm\,\varepsilon sm$

$\varepsilon sm=(\sigma s/Es)(1-\beta 1\beta 2(\sigma sr/\sigma s))$

$\sigma sr=(fctm\ Ac,ef)/As$

JSCE Formula

$Wmax = K1(4C+0.7(C\phi-\Phi))(\sigma se/Es+\varepsilon)$

All the calculated values are obtained using the stress in reinforcement under the dead load condition because the measured values are those of the dead load condition. However, the effects of loading history of live load on the crack width under dead load condition are very large and the corrosion of reinforcement is also affected by the crack width under live load condition, depending on the environmental condition and the way of using the member. Therefore, it is necessary to add a part or all of the live load to the dead load to decide the stress in reinforcement to be used in the calculation of crack width, depending on the requirement in the actual crack controlling design.

6. CONCLUSIONS

The following conclusions are reached through the comparison of the measurements and analyses of cracks in the tensile region of members in actual RC bridges with the test results about the axially tensioned prismatic RC specimens obtained by the authors.

(1) Both the crack density and the mean crack width in one meter in the tensile region of the actual RC girder gradually increase with the distance from the support toward the midspan. The increment of the values becomes fairly small beginning from a place at approximately a/d ((distance from the support)/(effective depth))=3.5.

(2) The distributions of crack spacings and crack widths in the tensile region of the actual RC girder conform not to the conventionally predicted normal distribution but to the logarithmic-normal distribution. This agrees with the findings by the authors through the experiment of axially tensioned RC specimens[1]. The reason is conceivably a great influence of the drying of concrete.

(3) According to the results of dynamic measurement of crack width on a T-section girder bridge, an increase in crack width of approximately 0.01~0.02 mm at midspan under train passing is observed. This is approximately 20 percent at most of the width under the dead load and it corresponds to an increase of approximately 30MPa in the stress of steel reinforcement. The reason for the small increase of crack width under live load is conceivably that the rigidity of the bridge is enlarged due to the existence of the slab track and road-bed concrete.

(4) Comparing the cracks in a box-girder between the eighth-month measurement before passing trains and the fifth-year measurement after passing trains, increases of 9 to 18 percent in the density and 13 to 38 percent in the mean width are recognized. These values are considerably larger than those of T-section girder in the same measurement period, that is approximately 3 percent in the density and 12 to 19 percent in the mean width. The box-girder which has thinner webs and slabs than T-section girder may be dried also from the inside.

(5) The relationship between the crack spacing and the crack width in the stable cracking condition is not such a simple linear relation as in the results obtained from the axially tensioned specimens. However, a relation of $W_{0.95}=aL+b$ holds between the crack spacing and 95 percent maximum crack width, $W_{0.95}$, though with some dispersion. The influence of drying on $W_{0.95}$ includes a component which affects L and a component which does not.

(6) Through the analysis of the measured results about actual RC bridges and the test results about axially tensioned specimens, a formula of L_{max} and W_{max} to be used for the crack controlling design of actual bridges has been obtained.

7.ACKNOWLEDGMENT

The authors extend sincere gratitude to Professor Yukimasa Goto at Tohoku Gakuin University for giving them precious advice on this study and to the staff of the Morioka Construction Bureau and the Track and Structural Department in the Sendai Railway Administration Bureau of Japanese National Railways for offering consistent cooperation.

References

[1] Y.Ozaka, K.Otsuka, and Y.Matsumoto: Cracks formed in Concrete Prism with Axial Tension Bars under Influence of Drying, Concrete Journal, Vol.23, No.3, 1985. (in Japanese)
[2] Y.Goto, S.Ueda, Y.Maki: Investigation on Tension Cracks in Reinforced Concrete Member -An Experiment by Tensile Bond Specimens-, Concrete Library of Japan Society of Civil Engineers, No.14, 1965. (in Japanese)
[3] Y.Goto, K.Otsuka: Experimental Studies on Cracks formed in Concrete around Deformed Tension Bars, Proceedings of JSCE, No.294, 1980.2. (in Japanese)
[4] Y.Kakuta: Maximum Crack Width in Reinforced Concrete, Concrete Journal, Vol.8, No.9, 1970.9. (in Japanese)

(Received 1986.12.25)